

Prediction of Organophosphorus Acetylcholinesterase Inhibition Using Three-Dimensional Quantitative Structure-Activity Relationship (3D-QSAR) Methods

Jamal El Yazal,* Shashidhar N. Rao,† Adrea Mehl,† and William Slikker, Jr.*¹

*Division of Neurotoxicology, National Center for Toxicological Research/FDA, 3900 NCTR Road, Jefferson, Arkansas, 72079; and

†Molecular Simulations, Inc., 9685 Scranton Road, San Diego, California 92121

Received May 10, 2001; accepted July 20, 2001

Neurotoxic organophosphorous compounds are known to modulate their biological effects through the inhibition of a number of esterases including acetylcholinesterase (AChE), the enzyme responsible for the degradation of the neurotransmitter acetylcholine. In this light, molecular modeling studies were performed on a collection of organophosphorous acetylcholinesterase inhibitors by the combined use of conformational analysis and 3D-QSAR methods to rationalize their inhibitory potencies against the enzyme. The Catalyst program was used to identify the structural features in the group of 8 inhibitors whose IC_{50} values ranged from 0.34 nM to 1.2 μ M. The 3-D pharmacophore models are characterized by at least one hydrogen bond acceptor site and 2–3 hydrophobic sites and demonstrate very good correlation between the predicted and experimental IC_{50} values. Our models can be useful in screening databases of organophosphorous compounds for their neurotoxicity potential *via* the inhibition of acetylcholinesterase. Also, the pharmacophores offer an additional means of designing AChE inhibitors as potential therapeutic agents for central nervous system diseases.

Key Words: 3-D pharmacophore; hypothesis; conformation; hydrophobic; hydrogen bond acceptor; insecticides.

The use of organophosphorus compounds (OPs) as insecticides represents a broad class of pesticides intensively applied to achieve household control of pests and enhanced agricultural production. Estimates of human exposures to OPs from occupational, dietary, household, and accidental/intentional situations have been reported in the tens of thousands to millions per year (Nigg *et al.*, 1990). The extensive application or misuse of these compounds results in deleterious health and potential safety hazards, including numerous documented cases of human fatalities (Wallace and Kemp, 1991; Wilkison, 1990).

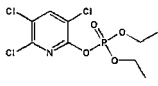
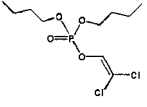
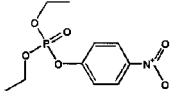
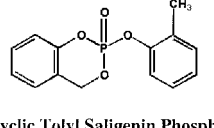
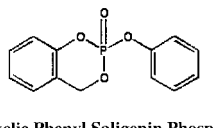
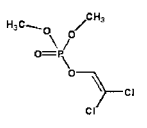
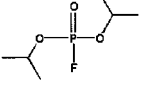

Acute poisoning by organophosphorus compounds presents a diverse spectra of sensitivity that varies according to the biological system or the species exposed (Andersen *et al.*,

1977; Johnson and Wallace, 1987; Lassiter *et al.*, 1999; Mileson *et al.*, 1998; Moser *et al.*, 1998; Murphy *et al.*, 1968; Wang and Murphy, 1982). Although the metabolism of OPs involves various enzymatic and pharmacokinetic pathways, the potential for toxicity in a species, induced by these compounds, largely depends on the inhibition of acetylcholinesterase (AChE) by the active oxygen analogue of the corresponding phosphorus triester (Wallace and Kemp, 1991). Binding affinity of the parent compound for AChE and/or its metabolic products is a major determinant of potency (Storm *et al.*, 2000).

The inhibition of AChE by OPs is sometimes followed by distinct chronic neurological consequences in exposed subjects. OPs cause various acute and subchronic neurotoxicity that ranges from chemical inhibition of AChE to alteration in spontaneous activity and sensory and neuromuscular performance (Mileson *et al.*, 1998). Chronic toxicity resulting from OP exposure ranges from cholinesterase inhibition in plasma, erythrocytes, and brain tissue to the appearance of clinical signs of long-term damage to the central nervous system (CNS) as well as peripheral nervous system (PNS; Durham and Ecobichon, 1986; Ecobichon *et al.*, 1990). AChE is known to be present in neuroblastoma cells (Ehrich *et al.*, 1997). Inhibition of AChE by OPs in neuroblastoma cells has been shown to correlate with acute neurotoxicity (Abou-Donia *et al.*, 2000; Ehrich *et al.*, 1997; Gorell *et al.*, 1998; Jett *et al.*, 1999; Jianmongkol *et al.*, 1996, 1999; Jortner *et al.*, 1999; Kellner *et al.*, 2000; Khan *et al.*, 2000; Mileson *et al.*, 1998; Padilla *et al.*, 2000; Pope *et al.*, 1995; Randall *et al.*, 1997; Richardson, 1995).

AChE catalyzes ester hydrolysis of the neurotransmitter acetylcholine, whose lowered levels are a feature associated with Alzheimer's disease (AD; Giacobini, 2000; Wang *et al.*, 1999). Hence, AChE inhibition is deemed a useful strategy in the design and development of drug candidates for the treatment of AD, as exemplified by the first approved drug, tacrine (Marquis, 1990). The duality of *in vivo* effects (beneficial and non-beneficial) of AChE inhibition make it important to understand the factors responsible for the specificity. In this

¹ To whom correspondence should be addressed. Fax: 870-543-7745. E-mail: wslikker@nctr.fda.gov.

Compound	IC ₅₀ (nM)	Number of conformations
 Chlorpyrifos-Oxon	0.34	183
 O,O-dibutyl O-(2,2-dichlorovinyl) Phosphate	0.94	186
 Paraoxon	2.3	40
 Cyclic Tofyl Saligenin Phosphate	28	14
 Cyclic Phenyl Saligenin Phosphate	260	7
 Dichlorvos	350	50
 Diisopropyl Phosphorofluoridate	190	16
 Trichlorfon	1200	77

study, the focus has been placed on some of the structural aspects of such factors.

In light of their significance, AChE and its inhibitors have been the target of numerous X-crystallographic (Axelsen *et al.*, 1994; Cygler *et al.*, 1993; Harel *et al.*, 1995, 1993; Silman *et al.*, 1994) and molecular modeling studies (Bernard *et al.*, 1999; Hirashima *et al.*, 2000; Hosea *et al.*, 1995, 1996; Inoue *et al.*, 1996; Kawakami *et al.*, 1996; Kovarik *et al.*, 1999; Pang and Kozikowski, 1994a,b; Pang *et al.*, 1996; Recanatini *et al.*, 2000; Silman *et al.*, 1999; Sussman *et al.*, 1993; van den Born *et al.*, 1995; Zeng *et al.*, 1999). Comparative QSAR analysis and 3-D docking studies on OP and non-OP compounds have been reported earlier (Bernard *et al.*, 1999; Hirashima *et al.*, 2000; Recanatini *et al.*, 1997). These studies have highlighted the role of the hydrophobic and electrostatic effects in the binding of the investigated compounds with the enzyme. The automated docking study reported by Bernard *et al.* (1999) concludes that aromatic and cationic leaving groups of the inhibitors are oriented toward the entry to the active site.

The X-ray crystal structures of AChE from different species have been documented in the protein data bank (e.g. Ieve, [Kryger *et al.*, 1999]). A number of ligands containing protonated amines have been co-crystallized with the enzyme. However, as none of the ligands found in the X-ray structure complexes belong to the organophosphorous group, no insights are available into the mechanism of their binding to the enzyme and consequently to their inhibitory effect. In order to understand the potential binding interactions of these compounds with the enzyme, we have carried out molecular modeling studies using 3-D pharmacophore modeling (3-D QSAR) on OPs, of which, the structures have been reported by Ehrich *et al.* (1997).

In this paper, we present the results of the 3-D QSAR studies. Herein, we have characterized the structural features essential for AChE inhibition by these compounds using the methods of 3-D QSAR. The 3-D models obtained feature at least 1 hydrogen bond acceptor pharmacophore and 2–3 hydrophobic interaction sites. The models demonstrate a high degree of correlation between the calculated and experimentally measured IC₅₀ values for AChE inhibition. Hence the models could be usefully employed to predict inhibitory potencies against AChE of a set of test compounds.

MATERIALS AND METHODS

Compounds 1–8 (Fig. 1) represent the members of the training set for the development of 3-D pharmacophores. These were drawn in 2D and converted to 3D using the Sketch-and-Converter module in Insight 2000 (Molecular Simulations Inc., San Diego, CA) and then energy minimized (using steepest

FIG. 1. Schematic illustration of 1–8 used in the development of 3-D pharmacophores to rationalize the AChE inhibitory activity. The IC₅₀ values (37°C, 1 h, Ehrich *et al.*, 1997) and the number of conformations generated for each compound are also indicated.

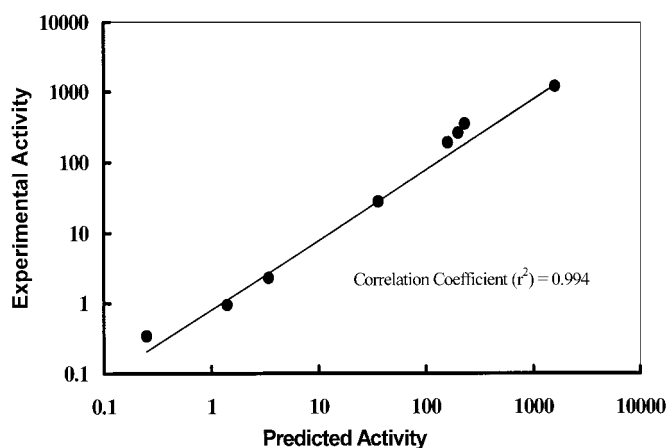


FIG. 2. Schematic illustration of the correlation plot between the predicted (from Hypothesis P1) and the experimentally measured IC_{50} against AChE.

descent and conjugate gradient algorithms) with the consistent-valence force field, CVFF. Subsequently, the structures were optimized using Merck Molecular modeling force field (MMFF) inside Cerius2 (version 4.5, Molecular Simulations, Inc.). The conformational analyses of 1–8 were carried out inside the Catalyst package (Molecular Simulations, Inc.). Conformations were generated using the “best” option (the program has the ability to modify the conformations of molecules during execution to provide a more precise database/spreadsheet search; the best algorithm finds the best fit among conformations, permitting no conformer’s energy to rise by more than the default value) with an energy cut-off of 15 kcal/mol. The maximum number of conformations to be generated for any molecule was set to 255. This is because Catalyst considers only the first 255 conformations in hypothesis generation (HypoGen; Li *et al.*, 1999). It may be noted that Catalyst generates random conformations (using a “polling” algorithm) to maximally span the accessible conformational space of a molecule and not necessarily *only* the local minima. In this light, the conformational models of the compounds will include some higher-energy structures that may be meaningful for receptor binding, since potentially favorable interactions (e.g., hydrogen bonding) with the latter will then compensate for the excessive conformational energy.

The conformational models of 1–8 (Fig. 1) were then imported into a Catalyst spreadsheet wherein their IC_{50} for the inhibition of AChE in SH-SY5Y human neuroblastoma cells were incorporated (Ehrich *et al.*, 1997). The selection of these IC_{50} values is based on the fact that all the OPs studied were examined under the same conditions, such as incubation temperature (37°C) and time of incubation (1 h). From the 11 agents reported by Ehrich *et al.* (1997), 8 were selected because of their rigid chemical conformation. Ehrich and coworkers also reported that this group of 8 agents exhibited adequate purity (100–87%). A value of 2.0 was employed for the “uncertainty factor.” This factor is an indicator of the accuracy in the experimentally measured data (highly reproducible data points will have an uncertainty factor close to 1.0).

Catalyst generates pharmacophore models based on structures and their corresponding activities. A pharmacophore can be defined as a 3-dimensional configuration of chemical features that is necessary for binding or modulating biological activity at a given receptor site. In Catalyst, feature-based pharmacophore models are generally referred to as hypotheses. Feature definitions are not limited to descriptions of specific chemical topology. Rather, they describe the kinds of interactions important for ligand-receptor binding.

Hypothesis models were generated, by requiring the presence of the following 3 features: hydrophobic, hydrogen bond acceptor, and ring aromatic. No restrictions were imposed on the presence of a minimum number of these features. Hypothesis models were generated using constant weights and constant tolerances on the features. In such hypotheses, all the potential pharmacophoric features were treated on par. For example, the hydrogen bond

acceptor feature was treated as no more or less important than the hydrophobic or ring aromatic feature. The resultant 3-D pharmacophore models were scored, ranked on the basis of their correlation factor, and analyzed for their cost factors. The correlation factor is indicative of the closeness of the predicted values of the dependent variable (biological activity) with respect to the experimentally measured values. Thus, a perfect correlation would correspond to a factor of 1.0.

The algorithm employed for Catalyst automatic hypothesis generation (hypoGen) will optimize hypotheses that are common to the active compounds in the training set, but not shared by the inactive compounds. This is done in 3 phases. In the constructive phase, hypotheses common to all actives are defined. The subtractive phase removes all hypotheses common to the inactive compounds. The third phase will optimize the resultant hypotheses from phase 2 that have survived the subtractive phase.

Catalyst uses bits for language, and will assign costs to hypotheses in terms of the number of bits required to describe them fully. During the beginning phase of an automated hypothesis generation, Catalyst calculates the cost of 2 theoretical hypotheses, 1 in which the error cost is minimal (all compounds fall along a line of slope = 1), and one where the error cost is high (all compounds fall along a line of slope = 0). These models can be considered upper and lower bounds for the training set. The cost values for them are useful guides for estimating the chances for a successful experiment.

The ideal hypothesis cost (fixed cost) tends to be 70–100 bits. The null hypothesis cost is usually higher than the fixed cost. The greater the difference between the fixed and the null costs, the higher the probability for finding useful models. In general, if the average costs of the generated hypotheses fall closer to the fixed cost, rather than the null hypothesis cost, then the hypotheses are considered more valid and worthy of evaluation.

Although Catalyst reports the top 10 hypothesis models by default, we have restricted our discussions to the top 4 models. For the sake of nomenclature, we have named the pharmacophore models as P1, P2, P3, and P4. Overlaps of various conformations of the molecules with the 3-D models were visualized in the *ViewHypothesis* workbench in Catalyst. All molecular simulations were carried out on a Silicon Graphics O2, running IRIX 6.5.

RESULTS AND DISCUSSION

Figure 1 lists the number of conformations for each of the 8 molecules in the training set. Their measured IC_{50} values for the inhibition of AChE range from 0.34 to 1200 nM. This spread of 4 orders of magnitude in the activity data make these compounds well suited for 3-D pharmacophore analyses using Catalyst. Each of the top 10 hypotheses reported by HypoGen is characterized by a correlation factor > 0.98. For the purposes of illustration, only the correlation plot between the

TABLE 1
The Predicted IC_{50} Values for the Training-Set Compounds Based on the Hypotheses P1, P2, P3 and P4

Mol. #	P1	P2	P3	P4	Exp IC_{50}
1	0.25	0.27	0.32	0.34	0.34
2	1.4	1.3	1.2	1.0	0.94
3	3.4	3.9	2.6	3.4	2.3
4	36	30	37	30	28
5	200	180	250	250	260
6	230	240	290	230	350
7	160	140	170	230	190
8	1900	2000	790	800	1200

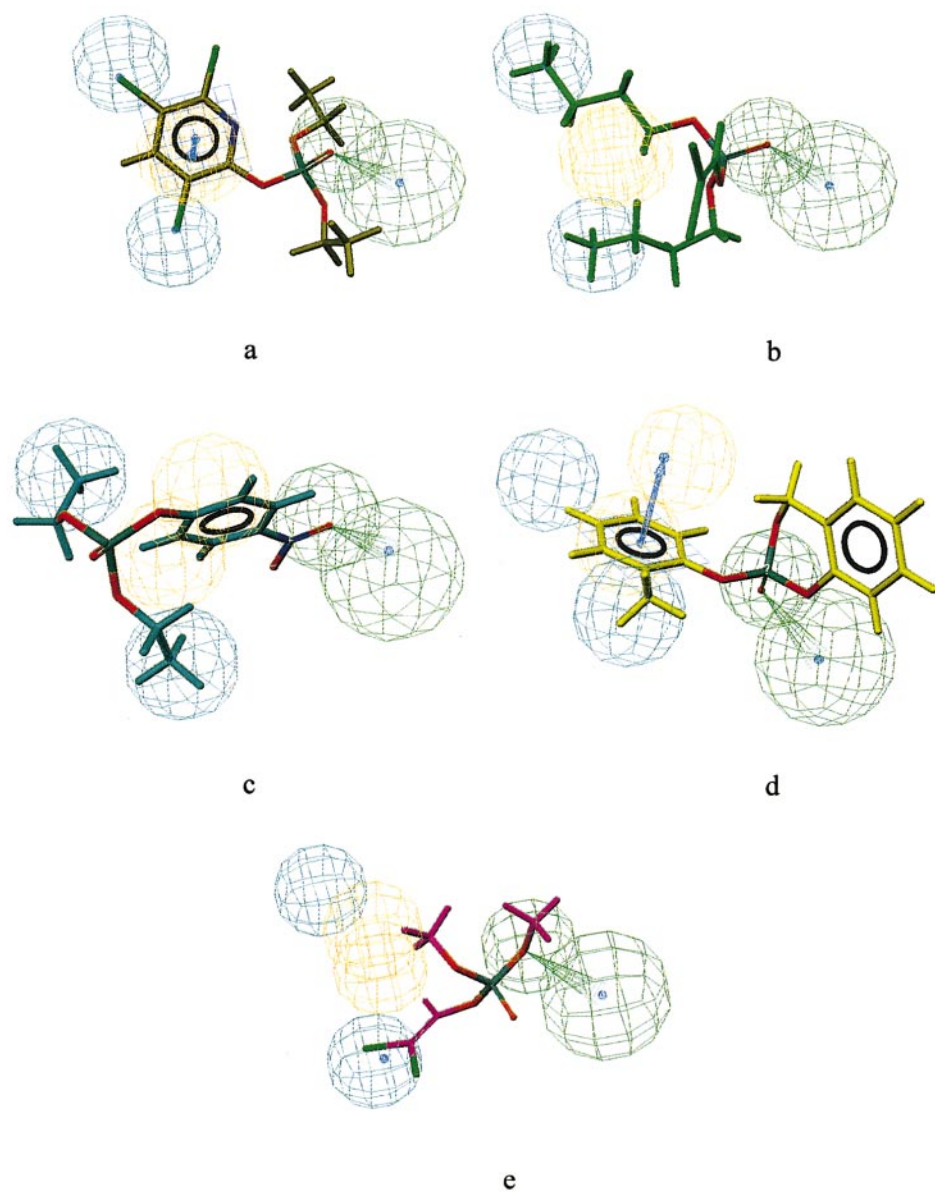


FIG. 3. (a) Shows a computer graphic illustration of the overlap of P1 with compound 1. (b) Shows that the hydrogen bond acceptor site (green) is occupied by the highly polarized phosphonyl oxygen. (c) Shows the absence of the normal to the ideal plane. (d) Shows the overlap of the less active compound 4 with P1. (e) Enables the understanding of the poor binding of compound 7 on the basis of poor occupation of the hydrophobic sites, non-occupation of the ring aromatic, and occupation of the hydrogen bonding-acceptor site by the less polar phosphoester oxygen.

experimentally measured and predicted IC_{50} values of P1 (correlation factor = 0.994) is graphically illustrated in Figure 2. The predicted IC_{50} values for the training set compounds based on the hypotheses P1, P2, P3 and P4 are shown in Table 1.

In addition, the hypotheses have been analyzed for various cost factors employed by Catalyst to identify the best hypotheses for a training set. The overall cost factor for each hypothesis is calculated by summing 3 cost factors: a weight cost, an error cost, and a configuration cost. The weight component is a value that increases in a gaussian form as the feature weight deviates from an ideal value (2.0). The error component increases as the root mean squared difference between estimated and measured activities for the training set molecules increases. The configuration component is a constant cost, which depends on the complexity of the hypothesized space being

optimized. It is equal to the entropy of the hypothesized space. In addition, fixed and null cost factors are computed for the hypotheses. The closeness of the overall cost factor to the fixed cost (representing the simplest model that fits the data in the training set perfectly) is indicative of the statistical significance of the hypothesis. The null cost factor corresponds to a theoretical hypothesis with no features that predicts the activity of every compound to be the average of all the activities. Hypotheses are deemed to be predictive in nature if the difference between the overall and null costs is at least 40 and the configuration cost factor (indicative of the entropy of the hypotheses space) is less than 17 (Guner *et al.*, 1991).

Figure 3a shows a computer graphic illustration of the overlap of P1 with compound 1. Two hydrophobic, 1 ring aromatic and 1 hydrogen bond acceptor feature characterize this hypoth-

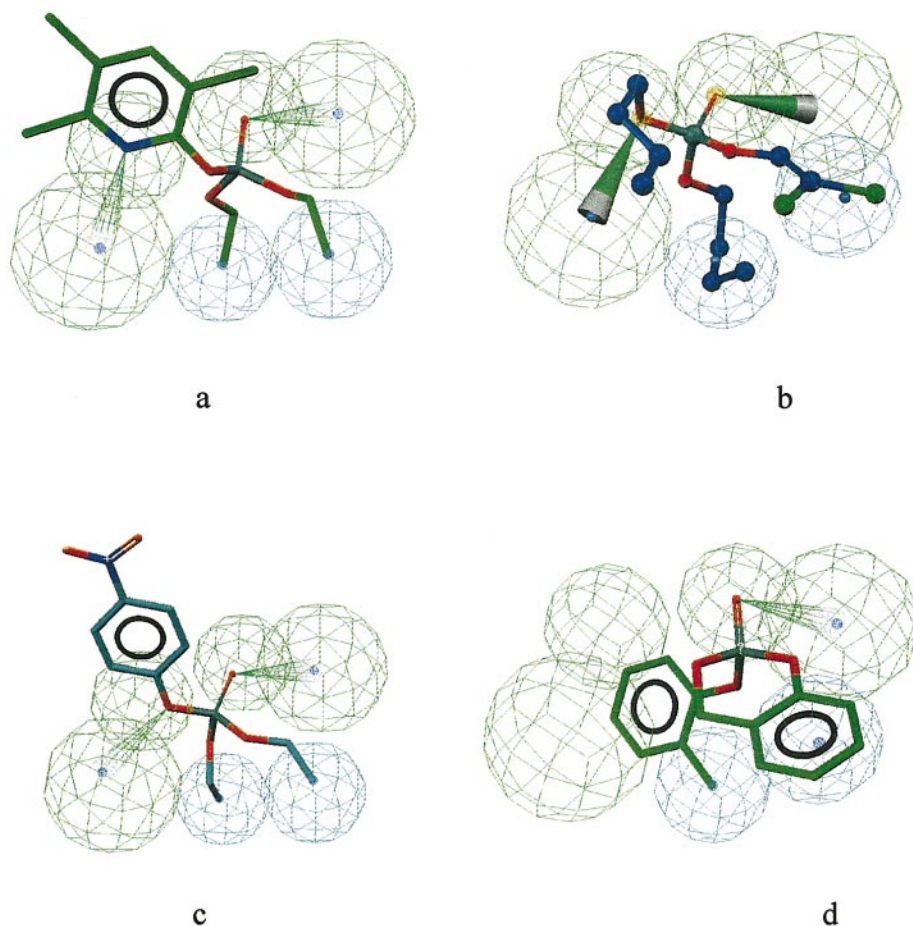


FIG. 4. Computer graphic illustrations of overlaps of the pharmacophore hypothesis P3 with compounds 1–4 (a–d, respectively).

esis model. The aromatic pyridine ring of 1 occupies the “ring aromatic” feature of this hypothesis. The 2 hydrophobic sites of the hypothesis are occupied by 2 chlorine atoms, which are attached to carbons 3 and 5 of the aromatic ring. The hydrogen bond-acceptor site (green) is occupied by the highly polarized phosphonyl oxygen. In the case of the overlap of P1 with 2 (Fig. 3b), the ring aromatic feature is unoccupied as the compound lacks an aromatic ring. As in 1, the phosphonyl oxygen occupies the hydrogen bond acceptor site, while the 2 hydrophobic sites are occupied by the terminal methyl groups of the 2 butoxy chains. The nitrophenyl compound 3 has its phenyl ring partially occupying the ring aromatic site. However, the plane of the aromatic ring is far removed from the ideal location as in the case of compound 1 (Fig. 3a), as evidenced by the absence of the normal to the ideal plane in Fig. 3c. Interestingly, the phosphonyl oxygen does not occupy the hydrogen-bonding site, which is engaged by 1 of the 2 oxygens in the nitro group. The overlap of the less active compound 4 with P1 is illustrated in Figure 3d. Here, the phosphonyl oxygen occupies the hydrogen bond-acceptor site, and the phenoxy phenyl occupies the ring aromatic site, with its normal lying very close in space to the ideal situation. One of the 2 hydrophobic sites remains unoccupied in this overlap. This is

suggestive of the potential for increased potency in this class of molecules with an additional hydrophobic substitution on the phenoxy phenyl group, *para* to the bridge oxygen. This overlap in Figure 3d also rationalizes the further reduced potency of compound 5 (260 nM), which lacks a methyl group on the phenoxy phenyl. In that case, both the hydrophobic sites of the hypothesis are not occupied. Figure 3e enables the understanding of the poor binding of compound 7 on the basis of poor occupation of the hydrophobic sites, non-occupation of the ring aromatic, and occupation of the hydrogen bonding-acceptor site by the less polar phosphoester oxygen.

Pharmacophore hypothesis P2 is qualitatively very similar to P1 and hence its overlaps with the members of the training set are not discussed. Hypotheses P3 and P4 are schematically illustrated in Figures 4a–d and Figures 5a–d, respectively, which show their overlaps with compounds 1–4. For both these hypotheses, the correlation with the experimental data is very strong, with an r -value of ~ 0.98 (Table 1). Just as in the case of P1, the predicted IC_{50} values lie within a factor of 2.0 relative to the experimental measurements.

Hypothesis P3 is characterized by 2 hydrophobic sites and 2 hydrogen bond-acceptor sites. Both acceptor sites are occupied in the case of overlaps with 1, 2, and 3. However, only 1 of

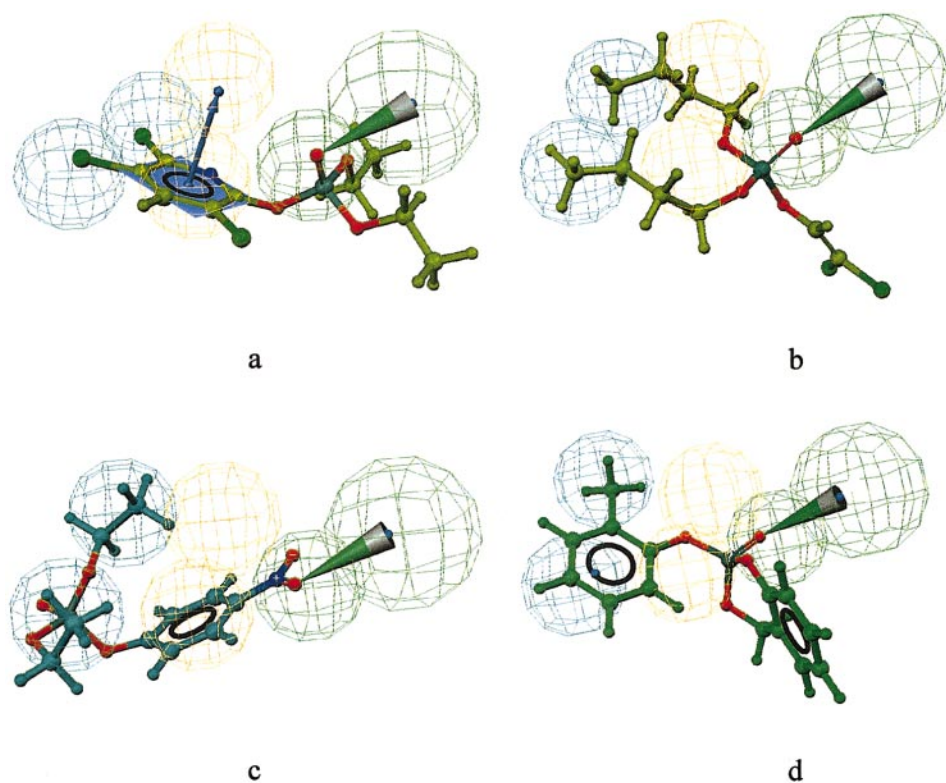


FIG. 5. Computer graphic illustrations of overlaps of the pharmacophore hypothesis P4 with compounds 1–4 (a-d, respectively).

them is occupied by a pendant phosphate oxygen in the conformationally constrained compound 4. The 2 hydrophobic sites in this hypothesis are occupied by appropriate groups in all the 4 compounds illustrated.

Hypothesis P4 is characterized by 2 hydrophobic sites, 1 hydrogen bond-acceptor site, and a ring aromatic site. This hypothesis thus has the same features as P1 and P2. However, the relative disposition of the features is different. Also, the ring aromatic feature is occupied only in the overlap with compound 1, but not in compounds 3 and 4, although they do contain a phenyl ring. Table 2 lists the lowest root mean square differences between the positions of the corresponding features in the 3 hypotheses P1, P2 and P4. A similar comparison with P3 is not meaningful as the latter has a different combination of features in it. Specifically, it lacks an aromatic ring feature and has an extra hydrogen bond acceptor feature.

TABLE 2

Root Mean Square Deviations in Angstroms between the 3 Hypotheses Containing Two Hydrophobic, an Aromatic Ring, and an H-Bond-Acceptor Feature

	P1	P2	P4
P1	0.0	1.72	1.92
P2	1.72	0.0	1.21
P4	1.92	1.21	0.0

Table 3 lists the cost factors associated with the 4 hypotheses discussed above. The configuration costs associated with these hypotheses (P1 through P4) are less than 17. The differences between the null hypothesis and the overall costs for P1 through P4 are around 50. These values imply the potential usefulness of the above pharmacophores as predictive models for estimating acetylcholinesterase inhibition activity of compounds outside the training set. In this light, we have carried out a search of the WDI (World Drug Index) 3-D database for compounds that are qualitatively consistent with P1 as an example, using the fast search strategy described earlier (Guner *et al.*, 1999). Compounds are deemed to be hits *only* when all the features contained in the pharmacophore hypothesis are

TABLE 3

Costs Associated with the Hypotheses P1 through P4

Hypothesis	Total	Error	Weight	Configuration
P1 to P4	39.39	23.22	1.12	15.05
P1 to P4	92.28	92.28	0	0
P1	40.36	24.03	1.29	15.04
P2	40.60	24.35	1.21	15.04
P3	41.06	23.65	2.36	15.04
P4	41.11	23.79	2.28	15.04

Note. Fixed costs are listed in the first line and null costs in the second line; the variable costs for each of the 4 hypotheses is given in the last 4 lines of the table.

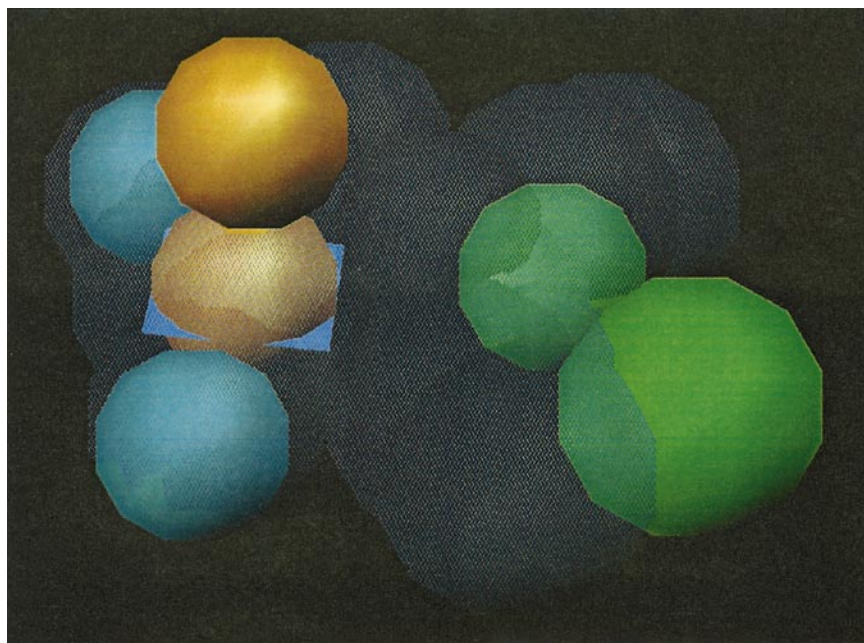


FIG. 6. Computer graphic illustration of the pharmacophore P1S represented by solid objects in cyan, green, and brown, superimposed with the shape query (gray) corresponding to the conformation of 1 in its overlap with P1.

present in the compound with the defined inter-feature spatial relationship. Database members with partial matches of the hypothesis are not deemed as hits. The results of the database search are discussed in the following section.

The choice of WDI is based in the fact that this database contains compounds of significant biological interest and it can be comparatively more useful to identify potential AChE inhibitors as compared to other equivalent databases such as ACD, NCI, Maybridge, etc. The search resulted in the identification of both OP and non-OP compounds from the database that share the 3-D pharmacophores exhibited by the OP compounds in their inhibition of AChE. The compounds identified as WDI hits are hypothesized to be AChE inhibitors based on their fit to the best pharmacophore obtained from the training set of compounds.

The 3-D Catalyst database of WDI with 49,661 compounds was initially screened for compounds with molecular weights between 200 and 500. This screen yielded a subset (referred to hereafter as SS1) of 32,831 compounds. Screening of SS1 against the hypothesis P1 using the fast flexible search method (using pre-computed conformations to model the flexibility of a molecule during a search; the fast algorithm finds the best fit among existing conformers) yielded the next subset SS2 of 16,216 compounds. In this method of database searching, compounds are identified as hits *only* when all the features in the hypothesis are present in their conformational models. The fit values (which measure how closely the functional groups in the hits match the feature centers) of the compounds in SS2 span the range of 0.5 to 8.3 for P1. The higher fit values indicate closer compatibility with the hypothesis model. Hence, compounds with fit values within the top 10% (between 7.4 and 8.3) and top 20% (between 6.2 and 8.3) brackets were listed in subsets SS3A (223) and SS3B (1668), respectively.

In light of the large number of hits obtained, further constraints were imposed by adding the shape of the conformation of the most active training-set compound (1) fitting to P1 (Fig. 3a) to the hypothesis. This ensures that the hits obtained not only contain all the features in the hypothesis, but also have a shape similar to the conformation of 1 as illustrated in Figure 3a. The shape-constrained hypothesis (P1S; graphically illustrated in Fig. 6) was screened against the subset SS3B to obtain a collection of 496 compounds (SS4) as hits. This subset was pruned further using the top 10% bracket of the fit values as the criterion, to obtain a list of 46 compounds (SS5) as the most likely ones to possess acetylcholinesterase inhibition activity. The WDI database was searched for compounds that had been screened and found to be active as AChE inhibitors. The database does not provide IC_{50} values, however. Nine hits were found (subset SS6). This did not include any of the compounds from SS5.

Members of SS6 were screened against P1 for their qualitative consistency with the 4-point pharmacophore. The fit values for these overlaps (Fig. 7a-i) are between 4.2 and 5.6 and their predicted IC_{50} values range from 9.3 nM (Fig. 7a) to 210 nM (Figs. 7f and 7g). Four of these compounds have molecular weights in excess of 500. Most of the 9 compounds were significantly larger in size and shape than the conformational model of 1 used in the determination-of-shape restraint (Fig. 7a-i). Also, in the overlaps of each of the 9 compounds, at most, 3 of the 4 pharmacophore features were occupied by corresponding functional groups in the molecules in SS6.

Limitations of the application of these findings to human toxicity need to be acknowledged. The source of the IC_{50} values from SH-SY5Y human neuroblastoma cells and purity of the OPs studied (100–87%, with all but 1 in the range of

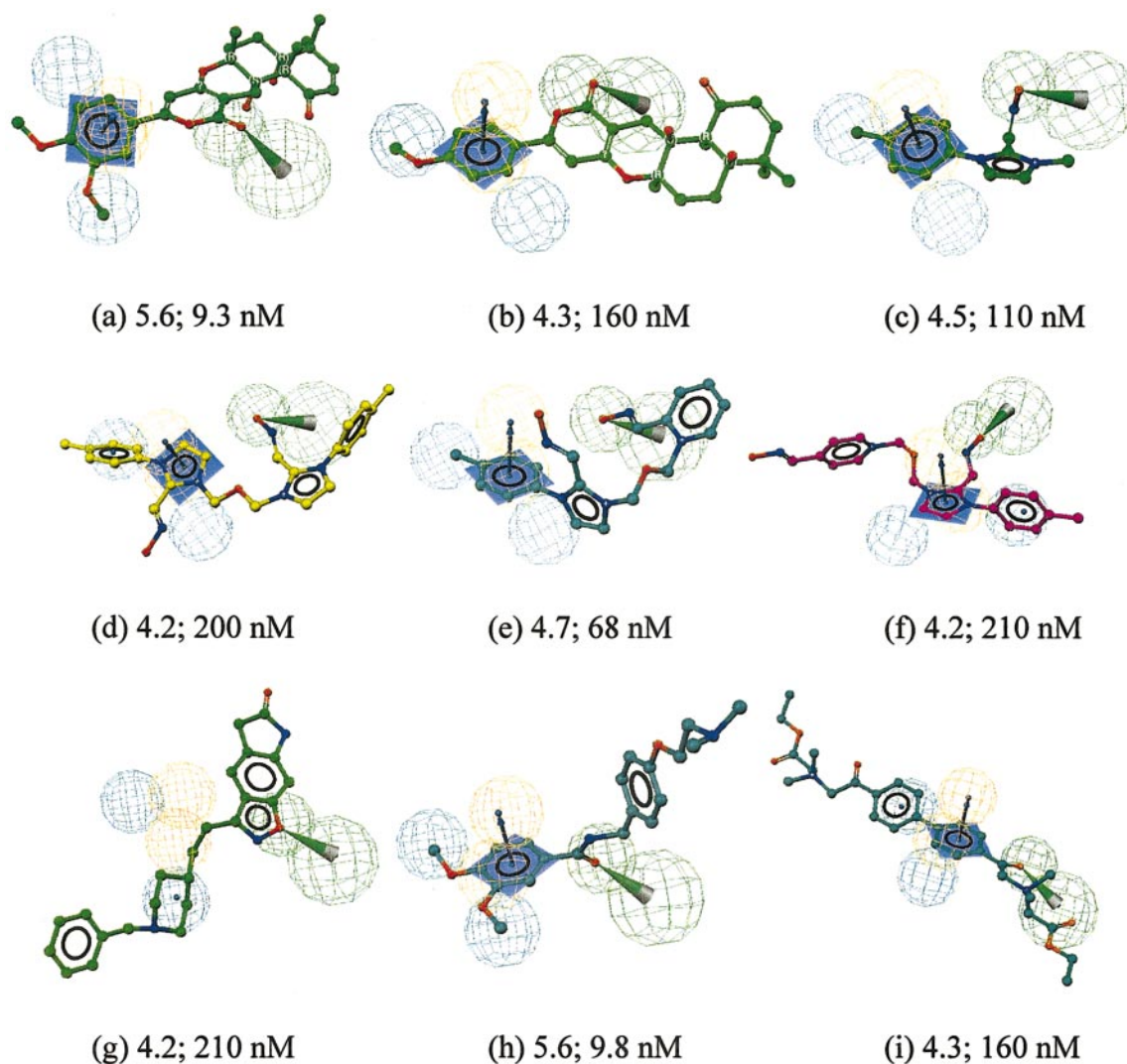


FIG. 7. Illustration of the overlaps of WDI compounds (assayed for AChE inhibition) with the pharmacophore P1. These are arisugacin-A (a), arisugacin-B (b), BMR-1 (c), BNR-2 (d), BMR-3 (e), BMR-4 (f), CP-118954 (g), itopride (h), and JGC-VII-110 (i). The fit values and the predicted IC_{50} values are also shown.

100–96% purity) may provide some uncertainty. However, as additional internally consistent IC_{50} data sets become available in the literature, collected from animal or human tissue, similar analyses can be completed and compared to the present findings.

X-ray structure analyses of complexes of acetylcholinesterases from different species with a number of inhibitors demonstrate that the bound ligand (with a cationic group) interacts with the enzyme through a water molecule in the active site. Typically, this is mediated through a hydrogen bond between the protonated amine (donor) of the ligand and the water oxygen (acceptor). Such water would in turn be hydrogen bonded to the protein residue. In light of this observation, it is interesting to speculate that the hydrogen bond-acceptor feature in the hypothesis model represents a moiety that interacts with the active-site water, which now acts as a hydrogen bond donor rather than as an acceptor, as in the X-ray structures.

Furthermore, the hydrophobic nature of the inhibitors promotes further interaction at the active site that is lined by the side chains of several large aromatic hydrophobic residues (e.g., Phe, Tyr). Thus, the AChE inhibition by the training set compounds 1–8 can be rationalized, even though they do not contain a potentially cationic group such as a tertiary or a secondary amine.

Conclusions

Three-dimensional pharmacophore models of phosphate-containing acetylcholinesterase inhibitors have been constructed using Catalyst to rationalize their inhibitory activity against acetylcholinesterase (AChE). The pharmacophore models demonstrate a high degree of correlation between the predicted and experimental data and are characterized by configuration costs (a measure of entropy in the hypotheses space)

of around 15, making them suitable for predictive purposes. All the models are characterized by at least 1 hydrogen bond-acceptor feature that typically corresponds to 1 of the phosphate oxygens in the molecules of the training set. This functional group, perhaps hydrogen bonds with a key active-site water molecule, leading to good binding as seen from the measured binding activity. A search of the WDI 3-D database yielded interesting small-molecule hits that do not belong to the class of organophosphorous compounds.

ACKNOWLEDGMENTS

This research was supported, in part, by a U.S. EPA/NCTR interagency agreement and by an appointment (J.E.Y.) to the Postdoctoral Research Program at the National Center for Toxicological Research, which is administered by the Oak Ridge Institute of Science and Education through an interagency agreement between the U.S. Department of Energy and the U.S. Food and Drug Administration.

REFERENCES

- Abou-Donia, M. B., Abdel-Rahman, A. A., Kishk, A. M., Walker, D., Markwiese, B. J., Acheson, S. K., Reagan, K. E., Swartzwelder, S., and Jensen, K. F. (2000). Neurotoxicity of ethyl methacrylate in rats. *J. Toxicol. Environ. Health* **59**, 97–118.
- Andersen, R. A., Aaraas, I., Gaare, G., and Fonnum, F. (1977). Inhibition of acetylcholinesterase from different species by organophosphorus compounds, carbamates, and methylsulphonyl fluoride. *General Pharmacology* **8**, 331–334.
- Axelsen, P. H., Harel, M., Silman, I., and Sussman, J. L. (1994). Structure and dynamics of the active site gorge of acetylcholinesterase: Synergistic use of molecular dynamics simulation and X-ray crystallography. *Protein Sci.* **3**, 188–197.
- Bernard, P., Kireev, D. B., Chretien, J. R., Fortier, P. L., and Coppet, L. (1999). Automated docking of 82 N-benzylpiperidine derivatives to mouse acetylcholinesterase and comparative molecular field analysis with 'natural' alignment. *J. Comput. Aided Mol. Des.* **13**, 355–371.
- Cygler, M., Schrag, J. D., Sussman, J. L., Harel, M., Silman, I., Gentry, M. K., and Doctor, B. P. (1993). Relationship between sequence conservation and three-dimensional structure in a large family of esterases, lipases, and related proteins. *Protein Sci.* **2**, 366–382.
- Durham, H. D., and Ecobichon, D. J. (1986). An assessment of the neurotoxic potential of fenitrothion in the hen. *Toxicology* **41**, 319–332.
- Ecobichon, D. J., Davies, J. E., Doull, J., Ehrich, M., Joy, R., McMillan, D., MacPhail, R., Reiter, L. W., Slikker, W., Jr., and Tilson, H. (1990). Neurotoxic effects of pesticides. In *The Effects of Pesticides on Human Health* (S. R. Baker and C. F. Wilkinson, Eds.), Vol. 18, pp.131–199. Princeton Scientific, Princeton, NJ.
- Ehrich, M., Correll, L., and Veronesi, B. (1997). Acetylcholinesterase and neuropathy target esterase inhibitions in neuroblastoma cells to distinguish organophosphorus compounds causing acute and delayed neurotoxicity. *Fundam. Appl. Toxicol.* **38**, 55–63.
- Giacobini, E. (2000). Cholinesterase inhibitors stabilize Alzheimer disease. *Neurochem. Res.* **25**, 1185–1190.
- Gorell, J. M., Johnson, C. C., Rybicki, B. A., Peterson, E. L., and Richardson, R. J. (1998). The risk of Parkinson's disease with exposure to pesticides, farming, well water, and rural living. *Neurology* **50**, 1346–1350.
- Guner, O. F., Hughes, D. W., and Dumont, L. M. (1991). An integrated approach to three-dimensional information management with MACCS-3D. *J. Chem. Inf. Comput. Sci.* **31**, 408–414.
- Guner, O. F., Waldman, M., Hoffmann, R. and Kim, J.-H. (2000). Strategies for database mining and pharmacophore development. In *Pharmacophore Perception, Development, and Use in Drug Design* (O. F. Guner, Ed.), pp. 213–236. IUL, La Jolla, CA.
- Harel, M., Kleywegt, G. J., Ravelli, R. B., Silman, I., and Sussman, J. L. (1995). Crystal structure of an acetylcholinesterase-fasciculin complex: Interaction of a three-fingered toxin from snake venom with its target. *Structure* **3**, 1355–1366.
- Harel, M., Schalk, I., Ehret-Sabatier, L., Bouet, F., Goeldner, M., Hirth, C., Axelsen, P. H., Silman, I., and Sussman, J. L. (1993). Quaternary ligand binding to aromatic residues in the active-site gorge of acetylcholinesterase. *Proc. Natl. Acad. Sci. U.S.A.* **90**, 9031–9059.
- Hirashima, A., Kuwano, E., and Eto, M. (2000). Docking study of enantiomeric fonofos oxon bound to the active site of Torpedo californica acetylcholinesterase. *Bioorg. Med. Chem.* **8**, 653–656.
- Hosea, N. A., Berman, H. A., and Taylor, P. (1995). Specificity and orientation of trigonal carboxyl esters and tetrahedral alkylphosphonyl esters in cholinesterases. *Biochemistry* **34**, 11528–11536.
- Hosea, N. A., Radic, Z., Tsigelny, I., Berman, H. A., Quinn, D. M., and Taylor, P. (1996). Aspartate 74 as a primary determinant in acetylcholinesterase governing specificity to cationic organophosphonates. *Biochemistry* **35**, 10995–10104.
- Inoue, A., Kawai, T., Wakita, M., Iimura, Y., Sugimoto, H., and Kawakami, Y. (1996). The simulated binding of (+/-)-2,3-dihydro-5,6-dimethoxy-2-[[1-(phenylmethyl)-4-piperidinyl]methyl]-1H-inden-1-one hydrochloride (E2020) and related inhibitors to free and acylated acetylcholinesterases and corresponding structure-activity analyses. *J. Med. Chem.* **39**, 4460–4470.
- Jett, D. A., Navoa, R. V., and Lyons, M. A., Jr. (1999). Additive inhibitory action of chlorpyrifos and polycyclic aromatic hydrocarbons on acetylcholinesterase activity in vitro. *Toxicol. Lett.* **105**, 223–229.
- Jianmongkol, S., Berkman, C. E., Thompson, C. M., and Richardson, R. J. (1996). Relative potencies of the four stereoisomers of isomalathion for inhibition of hen brain acetylcholinesterase and neurotoxic esterase in vitro. *Toxicol. Appl. Pharmacol.* **139**, 342–348.
- Jianmongkol, S., Marable, B. R., Berkman, C. E., Talley, T. T., Thompson, C. M., and Richardson, R. J. (1999). Kinetic evidence for different mechanisms of acetylcholinesterase inhibition by (1R)- and (1S)-stereoisomers of isomalathion. *Toxicol. Appl. Pharmacol.* **155**, 43–53.
- Johnson, J. A., and Wallace, K. B. (1987). Species-related differences in the inhibition of brain acetylcholinesterase by paraoxon and malaoxon. *Toxicol. Appl. Pharmacol.* **88**, 234–241.
- Jortner, B. S., Perkins, S. K., and Ehrich, M. (1999). Immunohistochemical study of phosphorylated neurofilaments during the evolution of organophosphorus ester-induced delayed neuropathy (OPIDN). *Neurotoxicology* **20**, 971–975.
- Kawakami, Y., Inoue, A., Kawai, T., Wakita, M., Sugimoto, H., and Hopfinger, A. J. (1996). The rationale for E2020 as a potent acetylcholinesterase inhibitor. *Bioorg. Med. Chem.* **4**, 1429–1446.
- Kellner, T., Sanborn, J., and Wilson, B. (2000). *In vitro* and *in vivo* assessment of the effect of impurities and chirality on methamidophos-induced neuropathy target esterase aging. *Toxicol. Sci.* **54**, 408–415.
- Khan, W. A., Dechkovskaia, A. M., Herrick, E. A., Jones, K. H., and Abou-Donia, M. B. (2000). Acute sarin exposure causes differential regulation of choline acetyltransferase, acetylcholinesterase, and acetylcholine receptors in the central nervous system of the rat. *Toxicol. Sci.* **57**, 112–120.
- Kovarik, Z., Radic, Z., Grgas, B., Skrinjaric-Spoljar, M., Reiner, E., and Simeon-Rudolf, V. (1999). Amino acid residues involved in the interaction of acetylcholinesterase and butyrylcholinesterase with the carbamates Ro 02–0683 and bambuterol, and with terbutaline. *Biochim. Biophys. Acta* **1433**, 261–271.
- Kryger, G., Silman, I., and Sussman, J. L. (1999). Structure of acetylcholinesterase

- terase complexed with E2020 (Aricept): Implications for the design of new anti-Alzheimer drugs. *Structure Fold. Des.* **7**, 297–307.
- Lassiter, T. L., Barone, S., Jr., Moser, V. C., and Padilla, S. (1999). Gestational exposure to chlorpyrifos: Dose-response profiles for cholinesterase and carboxylesterase activity. *Toxicol. Sci.* **52**, 92–100.
- Li, H., Sutter, J., and Hoffmann, R. (1999) Hypogen: An automated system for generating 3-D predictive pharmacophore models. *Pharmacophore Perception, Development and Use in Drug Design* (O. F. Guner, Ed.), pp. 171–189. IUL, La Jolla, CA.
- Marquis, J. K. (1990). Pharmacological significance of acetylcholinesterase inhibition by tetrahydroaminoacridine. *Biochem. Pharmacol.* **40**, 1071–1076.
- Milesion, B. E., Chambers, J. E., Chen, W. L., Dettbarn, W., Ehrich, M., Eldefrawi, A. T., Gaylor, D. W., Hamernik, K., Hodgson, E., Karczmar, A. G., Padilla, S., Pope, C. N., Richardson, R. J., Saunders, D. R., Sheets, L. P., Sultatos, L. G., and Wallace, K. B. (1998). Common mechanism of toxicity: A case study of organophosphorus pesticides. *Toxicol. Sci.* **41**, 8–20.
- Moser, V. C., Chanda, S. M., Mortensen, S. R., and Padilla, S. (1998). Age- and gender-related differences in sensitivity to chlorpyrifos in the rat reflect developmental profiles of esterase activities. *Toxicol. Sci.* **46**, 211–222.
- Murphy, S. D., Lauwerys, R. R., and Cheever, K. L. (1968). Comparative anticholinesterase action of organophosphorus insecticides in vertebrates. *Toxicol. Appl. Pharmacol.* **12**, 22–35.
- Nigg, H. N., Beier, R. C., Cattrer, O., Chaisson, C., Franklin, C., Lavy, T., Lewis, R. G., Lombardo, P., McCarthy, J. F., Maddy, K. T., Moses, M., Norris, D., Peck, C., Skinner, K., Tardiff, R. G. Exposure to pesticides. In *The Effects of Pesticides on Human Health* (S. R. Baker and C. F. Wilkinson, Eds.), Vol. 18, pp.135–130. Princeton Scientific, Princeton, NJ.
- Padilla, S., Buzzard, J., and Moser, V. C. (2000). Comparison of the role of esterases in the differential age-related sensitivity to chlorpyrifos and methamidophos. *Neurotoxicology* **21**, 49–56.
- Pang, Y. P., and Kozikowski, A. P. (1994a). Prediction of the binding site of 1-benzyl-4-[(5,6-dimethoxy-1-indanon-2-yl)methyl]piperidine in acetylcholinesterase by docking studies with the SYSDOC program. *J. Comput. Aided Mol. Des.* **8**, 683–693.
- Pang, Y. P., and Kozikowski, A. P. (1994b). Prediction of the binding sites of huperzine A in acetylcholinesterase by docking studies. *J. Comput. Aided Mol. Des.* **8**, 669–681.
- Pang, Y. P., Quiram, P., Jelacic, T., Hong, F., and Brimijoin, S. (1996). Highly potent, selective, and low cost bis-tetrahydroaminacrine inhibitors of acetylcholinesterase. Steps toward novel drugs for treating Alzheimer's disease. *J. Biol. Chem.* **271**, 23646–23649.
- Pope, C., diLorenzo, K., and Ehrich, M. (1995). Possible involvement of a neurotrophic factor during the early stages of organophosphate-induced delayed neurotoxicity. *Toxicol. Lett.* **75**, 111–117.
- Randall, J. C., Yano, B. L., and Richardson, R. J. (1997). Potentiation of organophosphorus compound-induced delayed neurotoxicity (OPIDN) in the central and peripheral nervous system of the adult hen: Distribution of axonal lesions. *J. Toxicol. Environ. Health* **51**, 571–590.
- Recanatini, M., Cavalli, A., Belluti, F., Piazzi, L., Rampa, A., Bisi, A., Gobbi, S., Valenti, P., Andrisano, V., Bartolini, M., and Cavrini, V. (2000). SAR of 9-amino-1,2,3,4-tetrahydroacridine-based acetylcholinesterase inhibitors: Synthesis, enzyme inhibitory activity, QSAR, and structure-based CoMFA of tacrine analogues. *J. Med. Chem.* **43**, 2007–2018.
- Recanatini, M., Cavalli, A., and Hansch, C. (1997). A comparative QSAR analysis of acetylcholinesterase inhibitors currently studied for the treatment of Alzheimer's disease. *Chem. Biol. Interact.* **105**, 199–228.
- Richardson, R. J. (1995). Assessment of the neurotoxic potential of chlorpyrifos relative to other organophosphorus compounds: A critical review of the literature. *J. Toxicol. Environ. Health* **44**, 135–165.
- Silman, I., Harel, M., Axelsen, P., Raves, M., and Sussman, J. L. (1994). Three-dimensional structures of acetylcholinesterase and of its complexes with anticholinesterase agents. *Biochemical Society Transactions* **22**, 745–749.
- Silman, I., Millard, C. B., Ordentlich, A., Greenblatt, H. M., Harel, M., Barak, D., Shafferman, A., and Sussman, J. L. (1999). A preliminary comparison of structural models for catalytic intermediates of acetylcholinesterase. *Chem. Biol. Interact.* **119–120**, 43–52.
- Storm, J. E., Rozman, K. K., and Doull, J. (2000). Occupational exposure limits for 30 organophosphate pesticides based on inhibition of red blood cell acetylcholinesterase. *Toxicology* **150**, 1–29.
- Sussman, J. L., Harel, M., and Silman, I. (1993). Three-dimensional structure of acetylcholinesterase and of its complexes with anticholinesterase drugs. *Chem. Biol. Interact.* **87**, 187–197.
- van den Born, H. K., Radic, Z., Marchot, P., Taylor, P., and Tsigelny, I. (1995). Theoretical analysis of the structure of the peptide fasciculins and its docking to acetylcholinesterase. *Protein Sci.* **4**, 703–715.
- Wallace, K. B., and Kemp, J. R. (1991). Species specificity in the chemical mechanisms of organophosphorus anticholinesterase activity. *Chem. Res. Toxicol.* **4**, 41–49.
- Wang, H., Carlier, P. R., Ho, W. L., Lee, N. T. K., Pang, Y. P., and Han, Y. F. (1999). Attenuation of scopolamine-induced deficits in navigational memory performance in rats by bis(7)-tacrine, a novel dimeric AChE inhibitor. *Acta Pharmacol. Sinica* **20**, 211–217.
- Wang, C., and Murphy, S. D. (1982). The role of non-critical binding proteins in the sensitivity of acetylcholinesterase from different species to diisopropyl fluorophosphate (DFP), *in vitro*. *Life Sciences* **31**, 139–149.
- Wilkinson, C. F. (1990). Introduction and Overview. In *The Effects of Pesticides on Human Health* (S.R. Baker and C.F. Wilkinson, Eds.), Vol. 18, pp. 5–33. Princeton Scientific, Princeton, NJ.
- Zeng, F., Jiang, H., Zhai, Y., Zhang, H., Chen, K., and Ji, R. (1999). Synthesis and acetylcholinesterase inhibitory activity of huperzine A-E2020 combined compound. *Bioorg. Med. Chem. Lett.* **9**, 3279–3284.